



HAL
open science

Geomorphology of the Beqaa Valley, Lebanon and Anti-Lebanon Mountains

Polina Lemenkova

► **To cite this version:**

Polina Lemenkova. Geomorphology of the Beqaa Valley, Lebanon and Anti-Lebanon Mountains. Acta Scientifica Naturalis, 2022, 9 (1), pp.1-22. 10.2478/asn-2022-0002 . hal-03649044

HAL Id: hal-03649044

<https://hal.science/hal-03649044>

Submitted on 22 Apr 2022

HAL is a multi-disciplinary open access archive for the deposit and dissemination of scientific research documents, whether they are published or not. The documents may come from teaching and research institutions in France or abroad, or from public or private research centers.

L'archive ouverte pluridisciplinaire **HAL**, est destinée au dépôt et à la diffusion de documents scientifiques de niveau recherche, publiés ou non, émanant des établissements d'enseignement et de recherche français ou étrangers, des laboratoires publics ou privés.



Distributed under a Creative Commons Attribution - NonCommercial - NoDerivatives 4.0 International License

Acta Scientifica Naturalis

Former Annual of Konstantin Preslavsky University of Shumen: Chemistry, Physics, Biology, Geography

Journal homepage: <https://content.sciendo.com/view/journals/asn/asn-overview.xml>

Geomorphology of the Beqaa Valley, Lebanon and Anti-Lebanon Mountains

Polina Lemenkova

*Université Libre de Bruxelles, École polytechnique de Bruxelles (Brussels Faculty of Engineering),
Laboratory of Image Synthesis and Analysis (LISA). Building L, Campus de Solbosch, Avenue Franklin
Roosevelt 50, Brussels 1000, Belgium*

Abstract: *Geomorphology of Lebanon presents a unique pattern of contrasting landforms. These include two notable mountain ranges, the Lebanon and Anti-Lebanon Mountains, the Beqaa Valley, the elongated coastal area and a significant amount of karst relief forms. This study focuses on the investigation of the topographic and geologic setting of Lebanon by visualizing datasets covering Lebanon and Anti-Lebanon mountains and the Beqaa Valley. Data were collected using the open source repositories of the high-resolution data (GEBCO, ETOPO1, DEM embedded in R). Three 3D models of the relief of the country are presented based on the 'grdview' package of GMT with azimuth rotations of the view point at 205°/30° and 165°/30°. The geologic map is based on the compiled datasets of the USGS. The R based modelling allowed division of the raster grid into several geomorphological zones according to the slope steepness and aspect orientation. The extreme elevations of the study area range from -2007 m and 2973 m. The key contribution of this work is the topographic and geologic data synthesis for 2D and 3D modelling of Lebanon. Another aspect concerns technical integration of GMT and R scripting approaches with QGIS mapping into the cartographic framework for visualizing of the Lebanese topography as a multi-tool approach. For the future similar studies on Lebanon this paper can serve as a guide for completing a project on the multi-source 2D and 3D data mapping as a conceptual foundation for research on Lebanese environment.*

Keywords: Lebanon, Beqaa, 3D visualization, cartography, GMT, R

Introduction

The study is focused on the cartographic visualization of the geomorphology of Lebanon. The study area is located in the east Mediterranean Sea, between the 33°–35°N and 35°–37°E (Fig. 1). Lebanon has a typical Mediterranean climate with a contrasted climate (e.g. temperature in winter/summer, intense precipitation in selected regions). The highlands of the Anti-Lebanon Mountains are notable for the relatively high precipitation gradually decreasing in eastward direction toward the Syrian Desert (Conard et al., 2013). However, local climate setting is currently experiencing rapid environmental changes including changes in precipitation and temperature (Cheddadi and Khater, 2016). Besides the climate factor, other impacts include socio-economic development and infrastructure (buildings, road systems), and touristic activities affecting the landscapes of the Mediterranean shores. Such correlations are reflected in previous studies on coastal zone management (Cori, 1999) and anthropogenic impact on the landscape patterns, e.g. deforestation and grazing (Hajar et al., 2010a).

In turn, climate variability in the Mediterranean Sea region regulates the distribution of vegetation. For instance, forest of *Cedrus libani* (A. Rich), precious cedar of Lebanon, a threatened conifer native to the Levant (Mouterde, 1983; Aziz, 1996; Bariteau, 2001), is currently experiencing shrinkage in its spatial distribution (Khuri et al., 2000; Hajar et al., 2010b), affected by both climate change and human activities. Likewise, *Pinus pinea* forests are also experiencing progressive disappearance (Nakhoul et al., 2020). Deep correlations between various landscape elements (mountains, hills, water bodies, rivers, lakes, land cover and land use enable to obtain information using datasets on related parameters (Jansen and Di Gregorio, 2004). Variations in landscape elements present various types of the ecological significance of habitats in natural ecosystems and are subject to monitoring (Klaučo et al., 2013a, 2013b; Lemenkova, 2013). At the same time, sustainable safeguarding of the precious environmental resources and landscapes, together with measures on conservation of the Lebanese biodiversity enable to provide cultural needs for the open/green spaces by the growing inhabitants of coastal cities of the country (Makhzoumi et al., 2012).

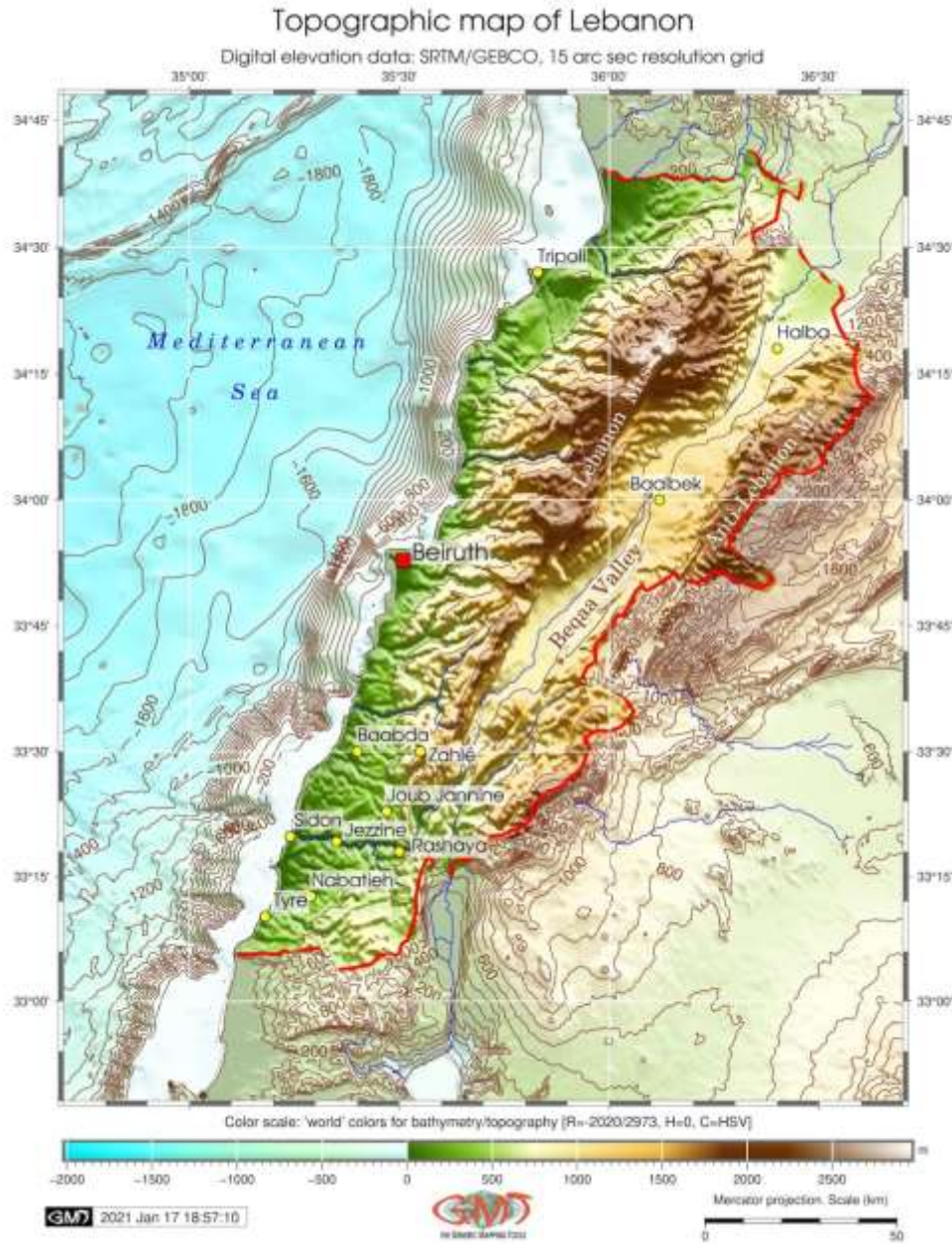


Figure 1. Topographic map of Lebanon. Data: GEBCO. Technique: clipped country area overprinted on the 60% transparent DEM image with isolines plotted every 100 m. Mapping: GMT. Source: author.

Topographical relief expressed in the dimensions of land surface is the prime factor controlling both human activities (construction of buildings and roads, infrastructure) and natural setting (vegetation distribution). Besides, the slope steepness of the terrain is one of the factors affecting possible geological hazards, such as landslides (Khawlie and Hassanain, 1984; Lemenkova et al., 2012). The relief of the region is generally expressed in local and regional geomorphological pattern with its derivatives: slope steepness,

aspect orientation and heights. Local variations in topography strongly affect the distribution of vegetation and hydrological network. In turn, they are being controlled by the geological setting of the region, its tectonic evolution and distribution of major geologic units and lineaments: faults, horsts, grabens. Regional geology reflects the processes of the orogenesis, as reported in details in publications on regional geology, active tectonics and seismicity of Lebanon (e.g. Walley, 1987, 1998; Carton et al., 2009).

Geologic setting of Lebanon is described and depicted on the existing consecutive series of geological maps at various scales (Dubertret, 1945, 1955, 1966, 1975; Davie, 1980). Its geology is studied by a variety of materials used for constructions and engineering: cement, concrete and pavement produced from Jurassic to Tertiary limestones, sands from Quaternary deposits, and Cretaceous sandstone formation, clays from the pockets within the basal Cretaceous units of Lebanon (Khawlie and Hinai, 1980).

In general, regional geologic evolution largely controls the landforms which reflect the distribution of the major geologic lineaments: faults, transform lines, tectonic plate borders (Lemenkova, 2019a, 2021a). Local geomorphological landforms in Lebanon are influenced by the distribution of the associated physical characteristics of rocks which includes porosity, density, pore type and size, textural parameters, elastic characteristics (Salah et al., 2020). In such a way they mirror lithological structure of the region. At the same time, physical rock properties control the distribution of the subsurface carbonate reservoirs and correlate with hydrodynamic properties of soils (Chalhoub et al., 2009).

A special topographic feature of Lebanon is karst, formed due to the favorable hydrogeologic conditions leading to the formation of carbonate rocks and large karst areas (Develle et al., 2011; Pasquier, 2010). For example, it is reported (Edgell, 1997) that over 67% of the area of Lebanon (around 6900 km²) is karstified. A large distribution of karst area is noted in thick, exposed, fractured and folded Jurassic, Cretaceous, and Eocene carbonates (Fig. 2), as well as in coastal Miocene limestones (Lamouroux, 1974; Alqudah et al., 2019; Maksoud et al., 2020). An important role in karst formation plays the increase of permeability and circulation of waters in the dolomitized zones ('pockets') within the limestone rocks of the Jurassic Kesrouane Formation (Nader et al., 2003). Coastal regions of Lebanon along the current coastline include a variety of minor geomorphological forms: beaches, dunes, beach-rocks and rocky limestone coasts (Abou el-Enin, 1973; Fleisch and Sanlaville, 1974; Nicod and Sanlaville, 1978).

The connections between the topography and bathymetry can further be well illustrated by the geomorphology, drainage systems and lithology in Lebanon that create conditions for the sediment transport into the eastern Mediterranean. For example, the geomorphologic system of submarine valleys provides natural paths for sediment transport from the adjacent land areas into the seafloor. Besides, it reflects regional geodynamic and tectonic setting (Beydoun, 1976; Lemenkova, 2020b, 2020c, 2021b; Gohl et al., 2006a, 2006b).

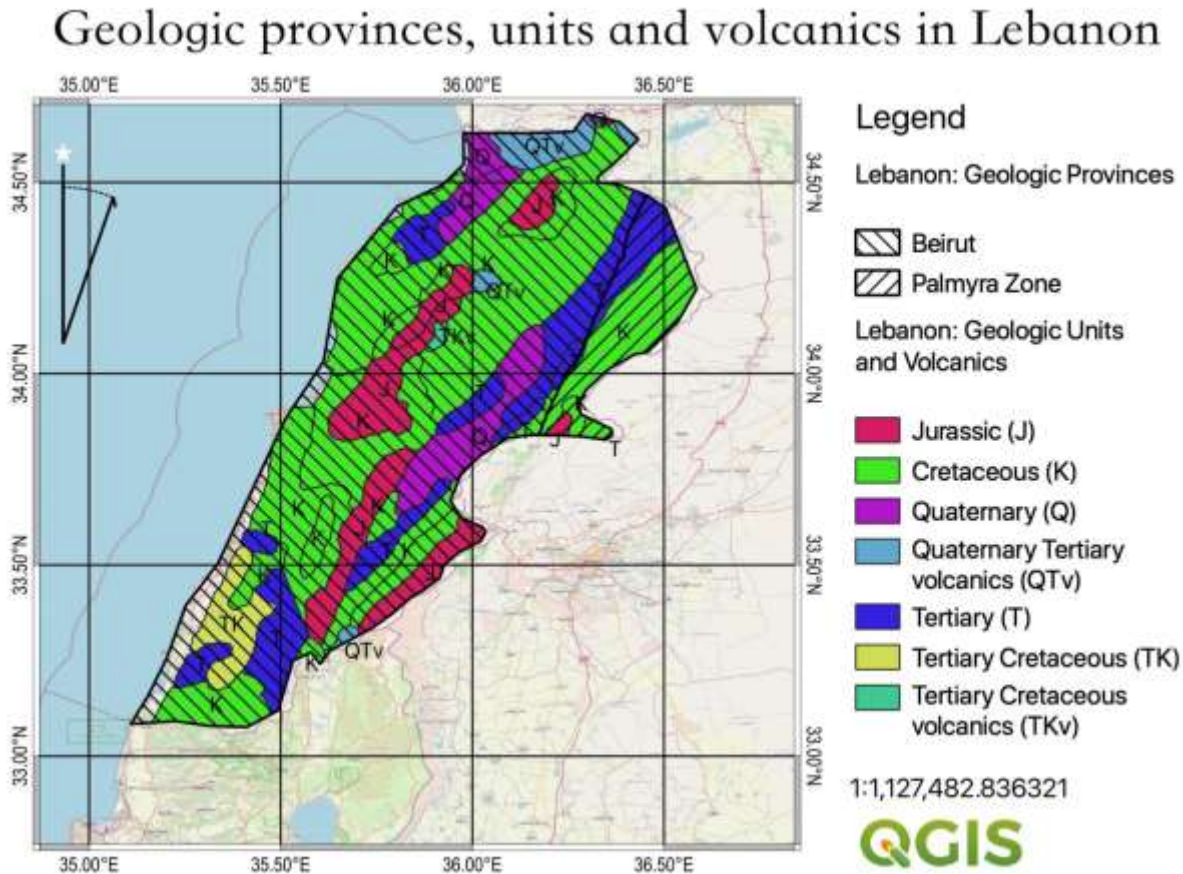


Figure 2. Geologic map of Lebanon (units, provinces and volcanics). Data: USGS .shp file overprinted on the OpenStreetMap tiles. Mapping: QGIS. Source: author.

The 3D cartographic visualization of the Lebanese topography is lacking, compared to the traditional existing thematic mapping of the country (Nicod and Sanlaville, 1978; ACSAD, 1985; Maalouf, 2008; Verdeil et al., 2016). At the same time, effective 2D and 3D visualization using advanced cartographic technologies highlights the importance of natural resources of the country both at regional and local levels (Lemenkov and Lemenkova, 2021). In many cases the existing papers on the high-resolution mapping using advanced cartographic solutions apply only to the specific topics of geology and topographic mapping (Heybroek, 1942; Butler and Spencer, 1999; Gauger et al., 2007; Lemenkova, 2013; Suetova et al., 2005). Other examples include technical papers on groundwater and hydrogeology (El-Fadel et al., 2001; Shaban, 2011, 2013; Shaban et al., 2013, 2021; Nassif, 2016), cartography and geoinformatics (Bou Kheir et al., 2014; Ichoku and Karnieli, 1996; Lemenkova, 2019c; Klaučo et al., 2014).

Despite the existing efforts to map geomorphology of Lebanon, some maps are outdated, while others are either printed in a monochrome palette and lower resolution or have special thematic focus. This raises a question of the cartographic update of the area using modern advanced technical tools. The combined visualization of Lebanon by means of GMT and R is still lacking. This paper aims to fill in the existing gap by using the modern tools of numerical cartography for visualization of the Lebanese terrain. Technical methods used in this study include scripting techniques and present a first attempt with a systematic approach of the 3D modelling of Lebanon using an integrated use of the GMT, QGIS and R.

Materials and Methods

1. Data

The data used in this study have high spatial resolution and compatibility with cartographic processing. Following types of data were downloaded from the open sources online repositories and used for the study:

- i) GEBCO topographic grid in 15 arc-second resolution (GEBCO Compilation Group (2020) used for plotting Fig. 1, 4 and 5;
- ii) Geological layers used for plotting Fig. 2 were obtained from the USGS open data (Pollastro et al., 1999);
- iii) ETOPO1 grid generated and compiled with 1 arc-minute resolution grid (Amante and Eakins, 2009) used for plotting Fig. 3;
- iv) DEM grid used for mapping geomorphometric models in Fig. 6 and Fig. 7 derived from the ‘raster’ library of R (Hijmans and van Etten, 2012).

The study area in Fig. 1 has been masked and overlaid on the neighboring countries with 60% transparency using the DCW layer (Digital Chart of the World) in GMT. This study was conducted in the area of Lebanon using a square mask of the study area at 34.7°/36.7° longitude easting and 32.8°/34.8° latitude northing.

2. Scripting in Generic Mapping Tools

The 3D modelling of the topography of Lebanon has been performed using Generic Mapping Tools (GMT) scripting toolset (Wessel et al., 2019). Several modules of GMT have been employed to perform topographic 2D and 3D modelling of Lebanon. The data were extracted from the general GEBCO grid by he module 'grdcut' using the coordinates: 'gmt grdcut GEBCO_2019.nc -R34.7/36.7/32.8/34.8 -Glb_relief.nc'. The 'pscoast' module enables to draw the countries borders and plot fluvial network, as well as to create a mask of vector layer from the DCW of country's polygon. The 'grdimage' module was used for plotting and visualizing the country using this code: 'gmt grdimage lb_relief.nc -Cmypalette.cpt -R34.7/36.7/32.8/34.8 -

JM6.5i -I+a15+ne0.75 -t60 -Xc -P -K > \$ps'. The 'psclip' module was used for clipping the area and overlaying it over the 60% transparent grid of the remaining image showing neighboring countries (Fig. 1).

The elevations heights in the digital grid serve as variables visualized using the 'world' (Fig. 1 and 5) and 'turbo' (Fig. 3 and 4) color palettes. The difference in the resolution grids of GEBCO (15 arc-minute) and ETOPO1 (1 arc-minute) is remarkably well illustrated by comparing Fig. 3 and 4 where the mesh plots visualize the same spatial extent modeled using different raster grids. The modeling itself has been performed using the following code snippet: 'gmt grdview lb_relief.nc -JM10c -R34.7/36.7/32.8/34.8 -JZ3.5c -Cpaulinep.cpt -p205/30 -Qsm -N-3500+glightgray -Wm0.07p -Wf0.1p,red -B0.5/0.5/2000:"Bathymetry and topography (m)":WeSZ -S5 -UBL/-10p/-12p -K > \$ps'.

Lebanon: 3D topographic mesh model based on ETOPO1 (1 arc minute resolution)

Perspective view, azimuth rotation: 205/30°

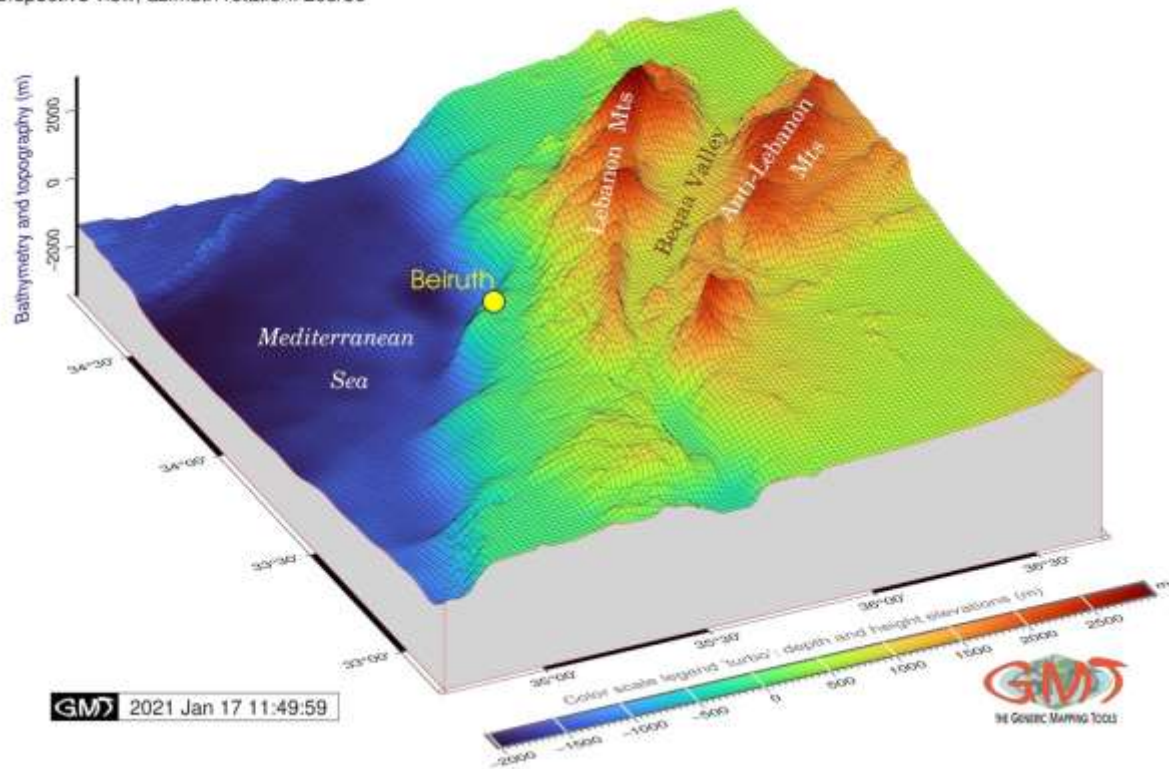


Figure 3. 3D model of Lebanon, rotation: 205°/30°. Data: ETOPO1. Source: author.

In this code each flag in the line of code indicates the specific cartographic elements, e.g. the '-R34.7/36.7/32.8/34.8' flag determines the region in WESN coordinates, the '-JZ3.5c' shows the z-dimension exaggeration, '-Qsm' defines the mesh plots, '-UBL' stamps the production date and time, '-Wm0.07p -Wf0.1p,red' define the color and size of the line contour, the '-JM10c' states the projection and physical

dimension of the map layout (Mercator, 10 cm plot), and the ‘-p205/30’ controls the rotation of the plot. Respectively, for the Fig. 5 the last flag has been changed to ‘-p165/30’. This explanation briefly illustrates the usage of GMT presented and explained technically in more details in the existing works (Lemenkova, 2019d, 2020d). The code written in GMT syntax uses a scheme equivalent to the programming languages and used as a tool for cartographic automatization (Lemenkova, 2019e; Schenke and Lemenkova, 2008). These lines of code were then combined in a script and re-used for plotting the 3D images in Fig. 3, 4 and 5 with changed rotation, raster grid and color palettes. The GMT includes a wide variety of types of modules, several of which were used to plot maps in Fig. 1, 3, 4 and 5. Hence, the codes were aggregated into a single script for each of the maps to visualize raster images that map viewers would presumably want to compare.

3. Mapping in QGIS

Mapping in QGIS (Fig. 2) has been performed using QGIS approach that includes the Graphical User Interface and menu and is compatible with the ArcGIS based format of the shape files (QGIS.org, 2021). This part of the study presents a qualitative visualization of the geologic vector layer made using import of the ArcGIS native format (.shp file) to the QGIS environment, and overlaid on the OpenStreetMap by the QGIS plugin. The map attempts to accumulate the existing geologic information on units, provinces and volcanics within the Lebanon using data captured from the USGS.

4. Modelling in RStudio

The geomorphometric modelling (Fig. 6 and 7) has been performed using R programming language (R Core Team, 2020) in RStudio environment (RStudio Team, 2017) using ‘raster’ and ‘tmap’ libraries (Tennekes, 2012) by the available techniques. Quantitative measurements and visualization of the geomorphometric parameters in different zones of the Lebanon and Anti-Lebanon mountains (Fig. 6 and 7) were done using ‘raster’ package of R based on DEM by RStudio using embedded algorithms of data processing in R. The geomorphometric analysis of terrain parameters of each site has been adopted after Doe (1971) and presented as calculations of slope and aspect and visualization of the hillshade and DEM. Slope steepness angle in 8 classes (North, East, South, West and their derivatives NE, NW, SE, SW), slope aspect, artificial illumination for the hillshade used for visualizing length of shadows with respect to area, DEM relief and elevations of the Lebanon and Anti-Lebanon Mountains and the Beqaa Valley were calculated using embedded DEM in a ‘raster’ package of R and visualized using ‘tmap’ library.

Lebanon: 3D topographic mesh model based on GEBCO (15 arc second resolution)

Perspective view, azimuth rotation: 205/30°

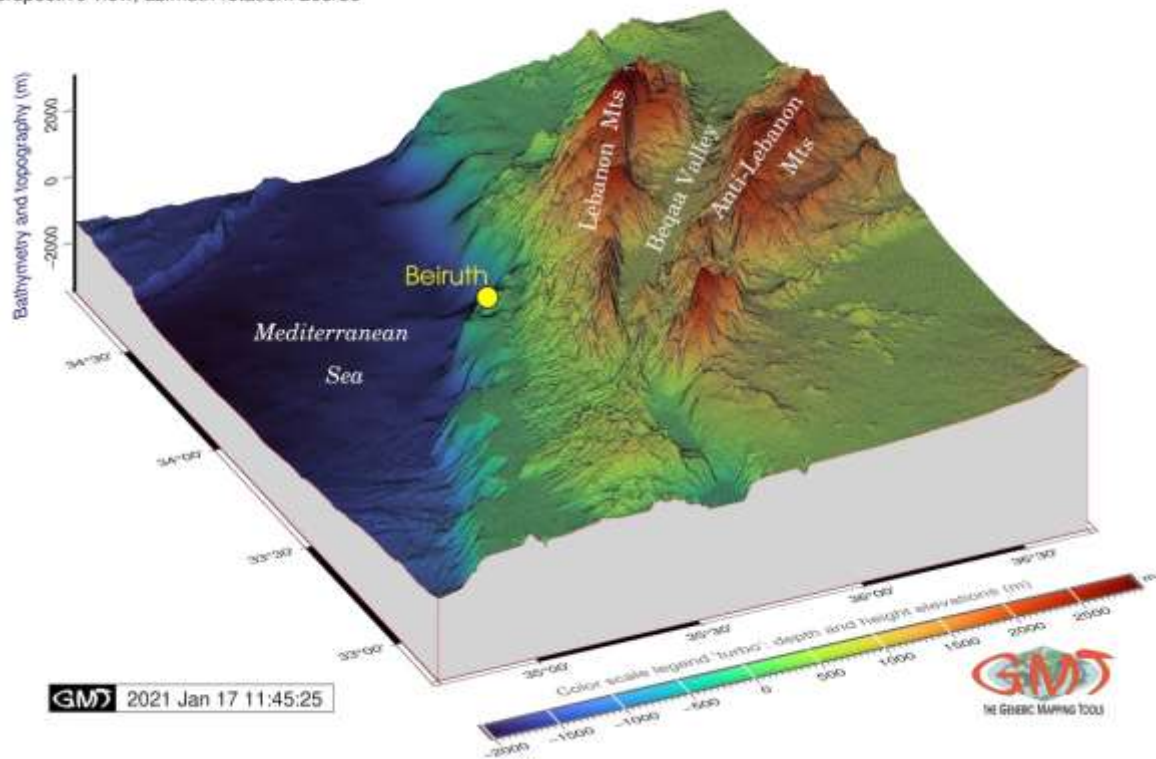


Figure 4. 3D model of Lebanon, rotation: 205°/30°. Data: GEBCO. Source: author.

The 'raster' package provided an access to the SRTM 90 m resolution elevation data with the `getData()` function using this code: `'alt = getData("alt", country = "Lebanon", path = tempdir())'`. Following that, the data were processed and modeled using special functionality of package: `'slope = terrain(alt, opt = "slope")'` and `'plot(slope)'`. The hillshade was calculated using parameters of angle at 40° and direction at 270° using the following code: `'hill = hillShade(slope, aspect, angle = 40, direction = 270)'`. Pairwise plotting of maps (slope-aspect, hillshade-elevation) using identical spatial extent and map projection enabled to illustrate the relationship between the geomorphometric parameters in the Lebanon and Anti-Lebanon Mountains.

Results and Discussion

Figure 1 shows the topography of the region visualized by GEBCO plotted using GMT. According to the GEBCO grid, the maximum and minimum elevation value above the sea level of the study area is -2007 m and 2973 m, respectively. The map illustrates the existence of a double mountain barrier (Lebanon Mountains and Anti-Lebanon Mountains) extending from S to N, rising from 2,000 to 2,973 m. The high plain of the Beqaa Valley is located between the two mountain ranges parallel to the coast.

Figure 2 illustrates the geologic setting of the region plotted using the QGIS. The output geologic map is created using the layout manager of the QGIS, to which a random color map suitable for categorical values is applied. Several cartographic elements (scale bar, north arrow, vertical legend and a main map) were adjusted to keep the layout readable using a background of the OpenStreetMap. The legend items include the outcrops of the Jurassic, Cretaceous, Quaternary and Tertiary geologic units of Lebanon, as well as two major provinces sub-dividing the country: the Beirut and the Palmyra. The Quaternary and tertiary units are subdivided into the sub-units, accordingly.

Figures 3, 4 and 5 shows the 3D visualization of the topography of Lebanon plotted using the ‘grdview’ module of GMT. The ranges of the Lebanon Mountains shown in Fig. 3 and 4 at the view of 205/30° is sculpturally visible on the 3D model highlighting the influence of tectonic structure on regional geomorphology, which is also pointed in a variety of relevant publications throughout the last several decades (see Veyret and Vaumas, 1955; Khair, 2001). Two grids (ETOPO1 and GEBCO) are remapped for the same territory and rotation azimuth (Fig. 3 and 4) using the two raster grids so that each demonstrates a difference between the topographic grids based on the GEBCO and ETOPO1 (Fig. 3 and 4), respectively.

The Figure 5 is plotted using 165/30° rotation azimuth aimed to show the 3D view of the country in the seaward orientation. The ranges of the Lebanon Mountains and Anti-Lebanon Mountains extend for approximately 160 km across the Lebanon, with a Beqaa Valley located in between, separating its coastland from the Syrian plain on the east, as also proved in previous notations (Klein, 2012) and is visible on the presented 3D models.

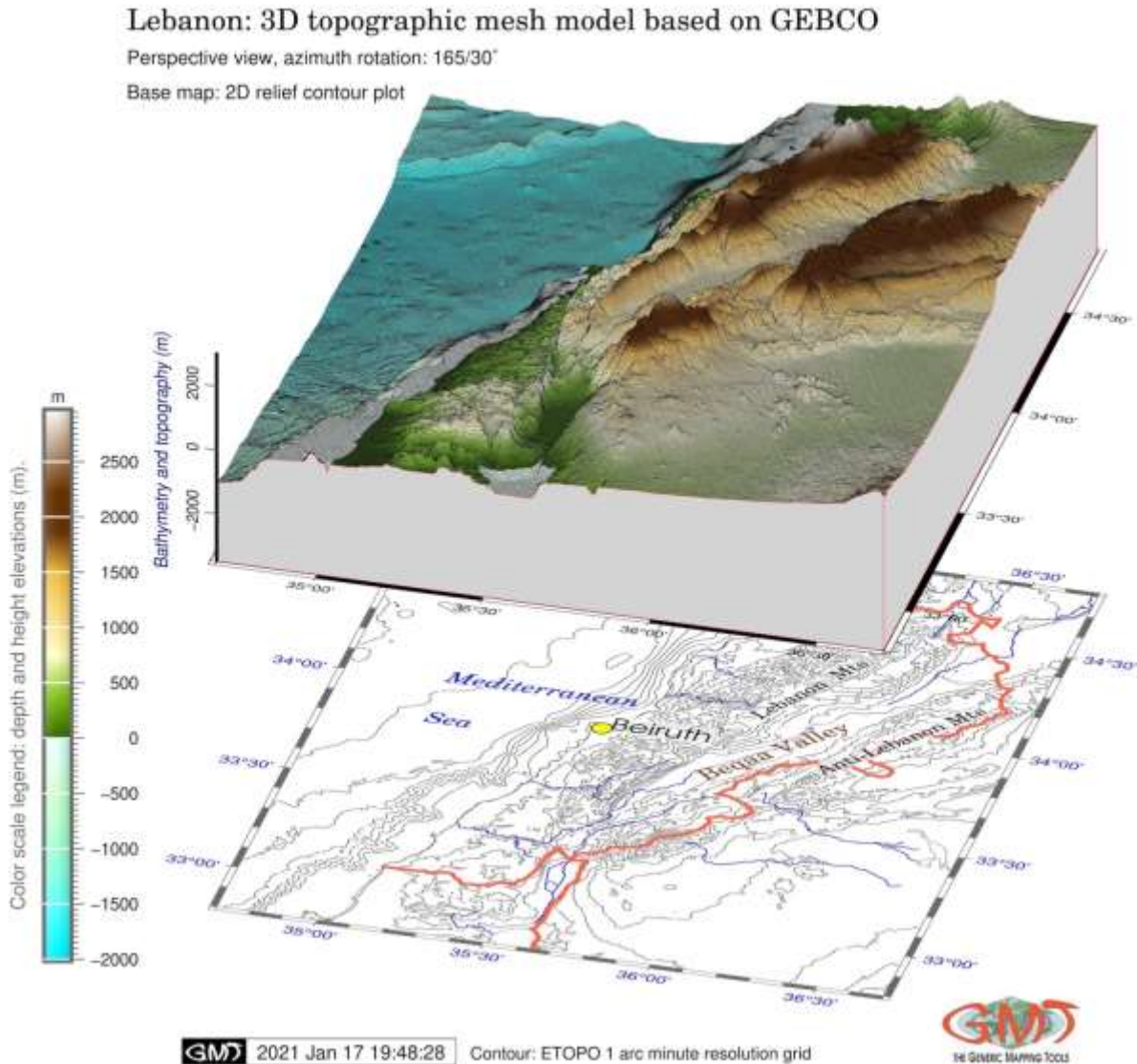


Figure 5. 3D model of Lebanon, rotation: 165°/30°. Data: GEBCO. Source: author.

Figure 6 is showing the slope (a) and aspect orientation (b) of the mountain ranges which illustrates the two important geomorphometric parameters of the mountains in the country. North-trending ranges of the high mountains of the country (Fig. 6) cause abundant precipitation and falls, including heavy rains and snowfalls on the mountains (Lebanon and Anti-Lebanon Mts) which, together with predominant calcareous lithology, contribute to the karstification in Lebanon.

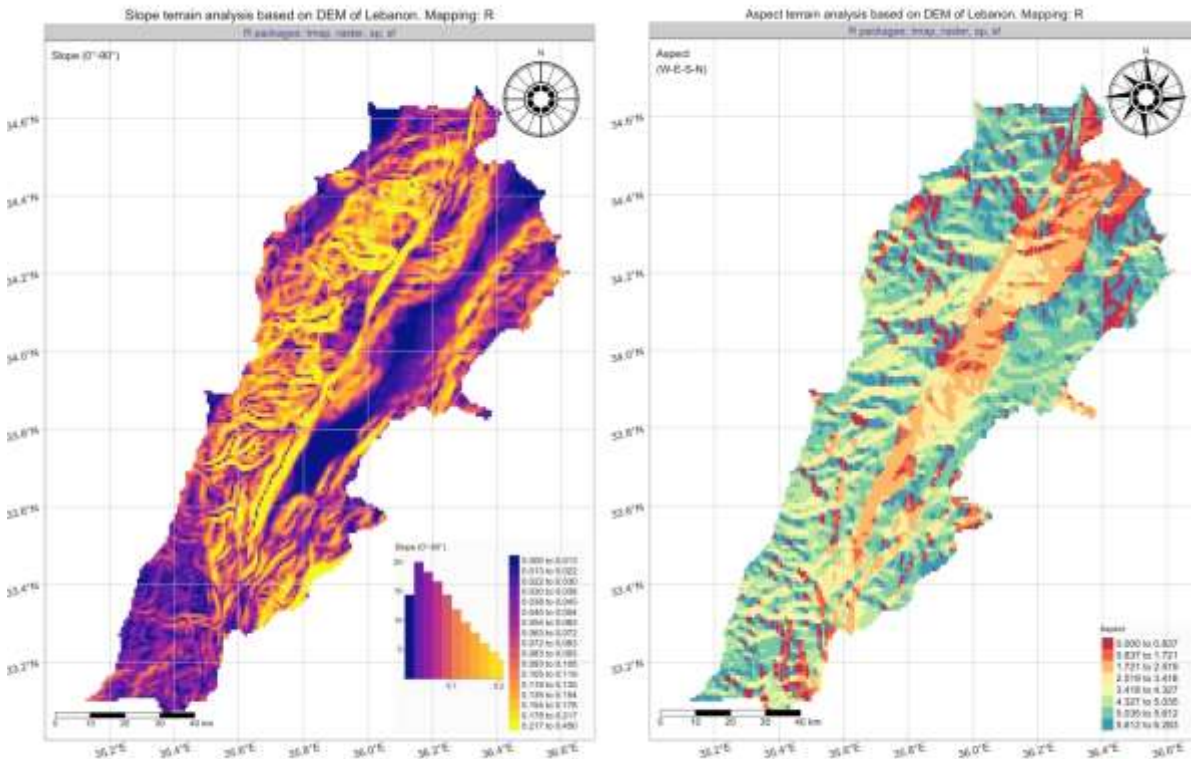


Figure 6. Slope and aspect terrain models of the DEM of Lebanon. Mapping: R. Source: author.

Figure 7 demonstrates the visualization of DEM (digital elevation model) of Lebanon and the hillshade view with artificially made illumination of the light source that stresses the topographic features. Local variations in topography (concave and convex meso- and microforms in the landforms) often control hydrological network through the surface runoff, may lead to local changes in soil type distribution and as a consequence, result in vegetation patterns affecting landscapes.

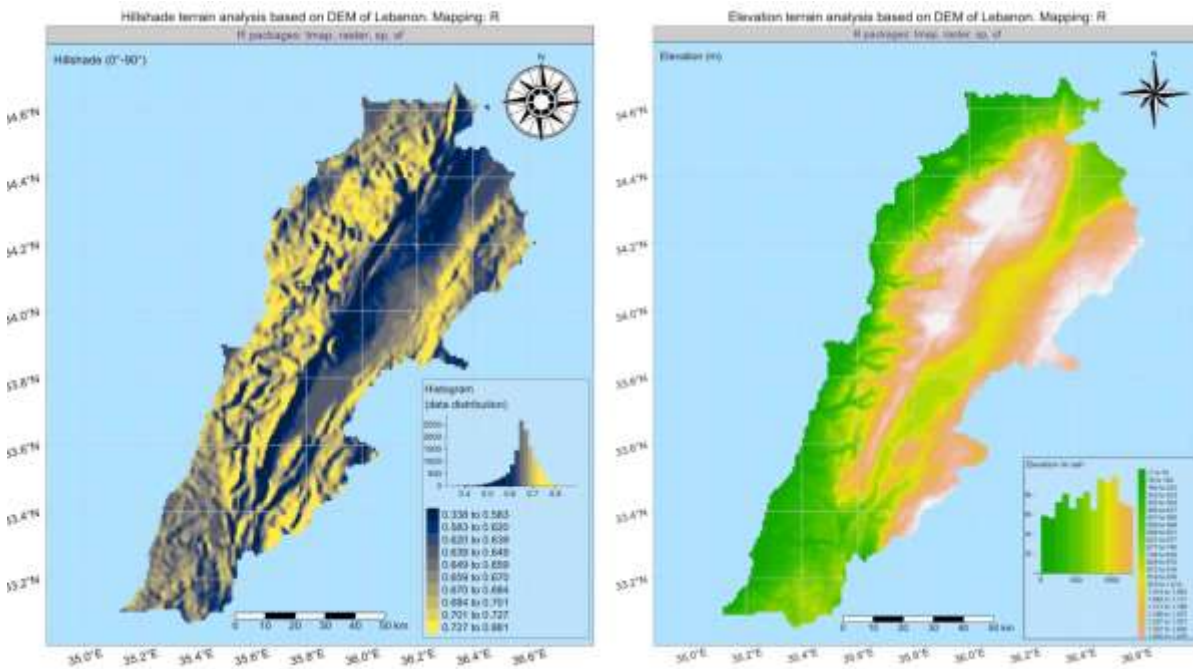


Figure 7. DEM elevation and hillshade models of Lebanon. Mapping: R. Source: author.

Conclusion

3D modelling is an effective tool for topographic visualization, modelling and representation of the landforms (Jaillet et al., 2019; Lemenkova 2020a, 2019b). Increasing the resolution of the geospatial data by selecting a finer grid is an important task when detailed information and accuracy are required. This paper presented the 3D topographic modelling using fine, middle and coarser resolution by the three different raster grids: GEBCO, ETOPO1 and DEM by R. Comparing these layers at different spatial resolutions used in cartographic representation and analysis of the topography of Lebanon, the finest resolution is demonstrated to be by GEBCO (Fig. 1, 4 and 5), while the middle resolution is presented by ETOPO1 (Fig. 3) and coarse resolution was used in R modelling: Fig. 6 a) and b) and 7, a) and b). This paper has presented work that has attempted to demonstrate the possibilities for practical visualization of several topographic maps demonstrating the relief of Lebanon in 2D and 3D using design approaches by the GMT and R scripting tools.

The methodology has been based on cartographic theoretical principles of data generalization and practical solutions by GMT scripting toolset and R language. Apart from the spatial data processing there has also been demonstrated cartographic art and design creativity in the presented map series. All the three resolutions can be applied for various tasks in spatial visualization of the Lebanese topography: the finest GEBCO-based data can be used for detailed geomorphological modelling and interpretations of the landforms at the local scale, the middle ETOPO1-based resolution can be utilized for mapping selected regional parts of

the country, and the coarser resolution of R can be used for general visualization of the relief used to highlight trends and orientation in the mountainous slopes.

Visualization of the Earth's surface and interpretation of the regional and local topography is important in various disciplines of the Earth sciences beyond technical mapping: geology, geomorphology, tectonics, soil and landscape studies, engineering geology and forest and vegetation monitoring and management. In response to the arising advances in technical approaches, many studies were published with data analysis, modelling and visualization (Jomaa, 2008; Jomaa et al., 2008; Klaučo et al., 2017; Awad et al., 2014; Jomaa and Khater, 2019; Lemenkova, 2011; Jomaa et al., 2019, Lemenkov & Lemenkova, 2021a, 2021b). This paper presented an application of combined approach of using R, GMT and QGIS for thematic mapping of Lebanon aimed at 2D and 3D visualization of its contrasting topographic setting. The paper demonstrated various 2D and 3D modeling methods by GMT, R and QGIS and Lebanese terrain analysis using 'raster' and 'tmap' packages and 'grdview' module of GMT.

The presented paper demonstrated that Lebanon has a specific contrasting topography including coastal areas, mountain ranges with varied slope steepness and spatial orientation and inter-mountainous valleys. The results are presented as a series of maps. The topographic features of Lebanon express the relief setting formed under the strong influence of endogenous factors (geologic history of the Earth) and exogenous factors (specific climate and environment of the Mediterranean Sea region). The variability of topography in Lebanon presented an excellent data for cartographic modelling, terrain analysis and visual interpretation. The paper presents new 7 maps and contributes to the regional studies of the topography of Lebanon and development of the cartographic methods of integrated 2D and 3D data processing.

Acknowledgement

The author cordially thanks the anonymous reviewers and the editor for the comments, remarks and editing of this manuscript.

References

- [1] Abou el-Enin, H.S., Essays on the geomorphology of the Lebanon, Beirut Arab University Press, P. 1 A, **1973**.
- [2] ACSAD, Soil Map of Arab Countries-Soil Map of Syria and Lebanon. The Arab Center for the Studies of Arid Zones and Drylands, Damascus, **1985**.
- [3] Alqudah, M.; Monzer, A.; Sanjuan, J.; Salah, M.K.; Alhejoj, I.K., Calcareous nannofossil, nummulite and ostracod assemblages from Paleocene to Miocene successions in the Bekaa Valley (Lebanon) and its

- paleogeographic implications, *Journal of African Earth Sciences*, **2019**, *151*, 82–94. <https://doi.org/10.1016/j.jafrearsci.2018.12.001>.
- [4] Amante, C.; Eakins, B.W., ETOPO1 1 Arc-Minute Global Relief Model: Procedures, Data Sources and Analysis. NOAA Technical Memorandum, 19, **2009**.
- [5] Awad, M.; Jomaa, I.; Arab, F., Improved Capability in Stone Pine Forest Mapping and Management in Lebanon Using Hyperspectral CHRIS-Proba Data Relative to Landsat ETM+, *Photogrammetric Engineering and Remote Sensing*, **2014**, *80*, 725–732.
- [6] Aziz, D., *Le Cèdre du Liban*, Beirut. Editions Arziates, Beirut, Lebanon, 24–31, **1996**.
- [7] Bariteau, M., Cèdres de l'Atlas et du Liban. In: E. Teissier du Cros (Ed.). Variétés forestières du futur. Réflexion à l'horizon 2020-2030, **2001**, hal-02826492, 67–69.
- [8] Beydoun, Z.R., Observations on geomorphology, transportation and distribution of sediments in western Lebanon and its continental shelf and slope regions, *Marine Geology*, **1976**, *21*(4), 311–324. [https://doi.org/10.1016/0025-3227\(76\)90013-X](https://doi.org/10.1016/0025-3227(76)90013-X).
- [9] Bou Kheir, R.; Shomar, B.; Greve, M.B.; Greve, M.H., On the quantitative relationships between environmental parameters and heavy metals pollution in Mediterranean soils using GIS regression-trees: The case study of Lebanon, *Journal of Geochemical Exploration*, **2014**, *147* (Part B), 250–259. <https://doi.org/10.1016/j.gexplo.2014.05.015>.
- [10] Butler, R.W.H.; Spencer, S., Landscape evolution and the preservation of tectonic landforms along the northern Yammouneh Fault, Lebanon, *Geological Society, London, Special Publications*, **1999**, *162*(1), 143. <http://dx.doi.org/10.1144/GSL.SP.1999.162.01.12>.
- [11] Carton, H.; Singh, S.C.; Tapponnier, P.; Elias, A.; Briais, A.; Sursock, A.; Jomaa, R.; King, G.C.P.; Daëron, M.; Jacques, E.; Barrier, L., Seismic evidence for Neogene and active shortening offshore of Lebanon (Shalimar cruise), *Journal of Geophysical Research*, **2009**, *114*, B07407. <https://doi.org/10.1029/2007JB005391>.
- [12] Chalhoub, M.; Vachier, P.; Coquet, Y.; Darwich, T.; Dever, L.; Mroueh, M., Caractérisation des propriétés hydrodynamiques d'un sol de la Bekaa (Liban) sur les rives du fleuve Litani, *Etude et Gestion des Sols*, **2009**, *16*(2), 67–84.
- [13] Cheddadi, R.; Khater, C., Climate change since the last glacial period in Lebanon and the persistence of Mediterranean species, *Quaternary Science Reviews*, **2016**, *150*, 146–157. <https://doi.org/10.1016/j.quascirev.2016.08.010>.
- [14] Conard, N.J.; Bretzke, K.; Deckers, K.; Masri, M.; Napierala, H.; Riehl, S.; Stahlschmidt, M.; Kandel, A.W., Natufian Lifeways in the Eastern Foothills of the Anti-Lebanon Mountains. In: Bar-Yosef, O. and F.R. Valla (Eds.). Natufian Foragers in the Levant – Terminal Pleistocene Social Changes in Western

- Asia. Chapter: Natufian Lifeways in the Eastern Foothills of the Anti-Lebanon Mountains, *International Monographs in Prehistory. Edition: Archaeological Series*, **2013**, 19, 1–16.
- [15] Cori, B., Spatial dynamics of Mediterranean coastal regions, *Journal of Coastal Conservation*, **1999**, 5, 105–112. <https://doi.org/10.1007/BF02802747>.
- [16] Davie, M.F., La cartographie géomorphologique au Liban. Inventaire et perspectives. Annales de Géographie de l'Université Saint-Joseph, Université Saint-Joseph, Beyrouth (Liban), **1980**, 1–26. hal-01078313.
- [17] Develle, A.-L.; Gasse, F.; Vidal, L.; Williamson, D.; Demory, F.; Van Campo, E.; Ghaleb, B.; Thouveny, N., A 250 ka sedimentary record from a small karstic lake in the Northern Levant (Yammoûneh, Lebanon): Paleoclimatic implications, *Palaeogeography, Palaeoclimatology, Palaeoecology*, **2011**, 305(1–4), 10–27. <https://doi.org/10.1016/j.palaeo.2011.02.008>.
- [18] Doe, J., Slope Aspect Determination, *Soil Survey Horizons*, **1971**, 12, 24–24. <https://doi.org/10.2136/sh1971.3.0024>.
- [19] Dubertret, L., Carte Géologique au 1:50,000, Feuille de Beyrouth, avec Notice Explicative. République Libanaise, Ministère des Travaux Publics, Beyrouth, 66 p., **1945**.
- [20] Dubertret, L., Carte géologique du Liban au 1:200,000 avec notice explicative. République Libanaise. Ministère des Travaux Publics, Beyrouth, 74 p., **1955**.
- [21] Dubertret, L., Liban, Syrie et bordure des pays voisins. Première partie. Tableau stratigraphique avec carte géologique au millionième, *Notes et Mém. Moyen-Orient*, **1966**, 8, 251–358.
- [22] Dubertret L., Introduction à la carte géologique à 1/50000 du Liban, *Notes et Mém. Moyen-Orient*, **1975**, 13, 345–403.
- [23] Edgell, H.S., Karst and hydrogeology of Lebanon, *Carbonates and Evaporites*, **1997**, 12(2), 220–235. <https://doi.org/10.1007/BF03175419>.
- [24] El-Fadel, M.; Zeinati, M.; Jamali, D., Water resources management in Lebanon: institutional capacity and policy options, *Water Policy*, **2001**, 3(5), 425–448. [https://doi.org/10.1016/S1366-7017\(01\)00079-4](https://doi.org/10.1016/S1366-7017(01)00079-4).
- [25] Fleisch, H.; Sanlaville, P., La plage de 52m et son acheuléen a Ras Beyrouth et a L'ouadi Aabet (Liban), *Paléorient*, **1974**, 2(1), 45–85. <http://www.jstor.org/stable/41489377>.
- [26] Gauger, S.; Kuhn, G.; Gohl, K.; Feigl, T.; Lemenkova, P.; Hillenbrand, C., Swath bathymetric mapping, *Reports on Polar and Marine Research*, **2007**, 557, 38–45. <https://doi.org/10.6084/m9.figshare.7439231>.
- [27] GEBCO Compilation Group, GEBCO 2020 Grid, **2020**. <https://doi.org/10.5285/a29c5465-b138-234d-e053-6c86abc040b9>.
- [28] Gohl, K.; Eagles, G.; Udintsev, G.; Larter, R.D.; Uenzelmann-Neben, G.; Schenke, H.-W.; Lemenkova, P.; Grobys, J.; Parsiegl, N.; Schlueter, P.; Deen, T.; Kuhn, G.; Hillenbrand, C.-D., Tectonic and

sedimentary processes of the West Antarctic margin of the Amundsen Sea embayment and Pine Island Bay, 2nd SCAR Open Science Meeting, 12–14 July 2006, Hobart, Australia, **2006a**. <https://doi.org/10.6084/m9.figshare.7435484>.

- [29] Gohl, K.; Uenzelmann-Neben, G.; Eagles, G.; Fahl, A.; Feigl, T.; Grobys, J.; Just, J.; Leinweber, V.; Lensch, N.; Mayr, C.; Parsiegla, N.; Rackebrandt, N.; Schlüter, P.; Suckro, S.; Zimmermann, K.; Gauger, S.; Bohlmann, H.; Netzeband, G.; Lemenkova, P., Crustal and Sedimentary Structures and Geodynamic Evolution of the West Antarctic Continental Margin and Pine Island Bay. *Expeditions programm Nr. 75 ANT XXIII/4 ANT XXIII/5*, **2006b**, 11–12. <https://doi.org/10.13140/RG.2.2.16473.36961>.
- [30] Hajar, L.; Haïdar-Boustani, M.; Khater, C.; Cheddadi, R., Environmental changes in Lebanon during the Holocene: Man vs. climate impacts, *Journal of Arid Environments*, **2010a**, 74(7), 746–755. <https://doi.org/10.1016/j.jaridenv.2008.11.002>.
- [31] Hajar, L., François, L.; Khater, C.; Jomaa, I.; Déqué, M.; Cheddadi, R., *Cedrus libani* (A. Rich) distribution in Lebanon: Past, present and future, *Comptes Rendus Biologies*, **2010b**, 333(8), 622–630. <https://doi.org/10.1016/j.crv.2010.05.003>.
- [32] Hijmans, R.J.; van Etten, J., raster: Geographic analysis and modeling with raster data, R package version 2.0-12, **2012**. <http://CRAN.R-project.org/package=raster>.
- [33] Heybroek, F., La géologie d'une partie du Liban Sud, *Leidse geologische mededelingen*, **1942**, 12, 251–470.
- [34] Ichoku, C.; Karnieli, A., A review of mixture modeling techniques for sub-pixel land cover estimation, *Remote Sensing Reviews*, **1996**, 13(3–4), 161–186. <https://doi.org/10.1080/02757259609532303>.
- [35] Jaillet, S.; Delannoy, J.-J.; Génuite, K.; Hobléa, F.; Monney, J., L'image topographique du karst et des grottes: représentations 2D et technologies 3D, entre réalité et imaginaire, *Géomorphologie, relief, processus, environnement*, **2019**, 25(3). <https://doi.org/10.4000/geomorphologie.13488>.
- [36] Jansen, L.J.M.; Di Gregorio, A., Obtaining land-use information from a remotely sensed land cover map: results from a case study in Lebanon, *International Journal of Applied Earth Observation and Geoinformation*, **2004**, 5(2), 141–157. <https://doi.org/10.1016/j.jag.2004.02.001>.
- [37] Jomaa I., Analyse diachronique de la fragmentation des forêts du Liban, Thesis, Université Paul Sabatier, Toulouse, **2008**.
- [38] Jomaa, I.; Auda, Y.; Abi Saleh, B.; Hamze, M.; Safi, S., Landscape Spatial Dynamics over 38 Years under Natural and Anthropogenic Pressures in Mount Lebanon, *Landscape and Urban Planning*, **2008**, 87, 67–75. <https://doi.org/10.1016/j.landurbplan.2008.04.007>.

- [39] Jomaa, I.; Khater, C., Mapping Glitches of Juniper Forests in Lebanon under Natural Conditions and Anthropogenic Activities, *Open Journal of Forestry*, **2019**, 9, 168–181. <https://doi.org/10.4236/ojf.2019.92008>.
- [40] Jomaa, I.; Saab, M.T.A.; Skaf, S.; El Haj, N.; Massaad, R., Variability in Spatial Distribution of Precipitation Overall Rugged Topography of Lebanon, Using TRMM Images, *Atmospheric and Climate Sciences*, **2019**, 9, 369–380. <https://doi.org/10.4236/acs.2019.93026>.
- [41] Khair, K., Geomorphology and seismicity of the Roum Fault as one of the active branches of the Dead Sea Fault System in Lebanon, *Journal of Geophysical Research*, **2001**, 106(B3), 4233–4245. <https://doi.org/10.1029/2000JB900287>.
- [42] Khawlie, M.R.; Hinai, K., Geology and production of construction material resources of Lebanon: a preliminary study, *Engineering Geology*, **1980**, 15(3–4), 223–232. [https://doi.org/10.1016/0013-7952\(80\)90036-8](https://doi.org/10.1016/0013-7952(80)90036-8).
- [43] Khawlie, M.R.; Hassanain, H.I., Engineering geology of the Hammana landslides, Lebanon, *Quarterly Journal of Engineering Geology and Hydrogeology*, **1984**, 17(2), 137. <http://dx.doi.org/10.1144/GSL.QJEG.1984.017.02.05>.
- [44] Khuri, S., Shmoury, M.; Baalbaki, R.; Maunder, M.; Talhouk, S.N., Conservation of the Cedrus Libani populations in Lebanon: History, current status and experimental application of somatic embryogenesis, *Biodiversity and Conservation*, **2000**, 9, 1261–1273. <https://doi.org/10.1023/A:1008936104581>.
- [45] Klaučo, M., Gregorová, B.; Stankov, U.; Marković, V.; Lemenkova, P., Determination of ecological significance based on geostatistical assessment: a case study from the Slovak Natura 2000 protected area, *Open Geosciences*, **2013a**, 5(1), 28–42. <https://doi.org/10.2478/s13533-012-0120-0>.
- [46] Klaučo, M., Gregorová, B.; Stankov, U.; Marković, V.; Lemenkova, P., Interpretation of Landscape Values, Typology and Quality Using Methods of Spatial Metrics for Ecological Planning. – In: *Environmental and Climate Technologies*, October 14, 2013. Riga, Latvia, **2013b**. <https://doi.org/10.13140/RG.2.2.23026.96963>.
- [47] Klaučo, M., Gregorová, B.; Stankov, U.; Marković, V.; Lemenkova, P., Landscape metrics as indicator for ecological significance: assessment of Sitno Natura 2000 sites, Slovakia. In: *Ecology and Environmental Protection*. March 19–20, 2014, Minsk, Belarus, 85–90, **2014**. <https://doi.org/10.6084/m9.figshare.7434200>.
- [48] Klaučo, M., Gregorová, B.; Koleda, P.; Stankov, U.; Marković, V.; Lemenkova, P., Land planning as a support for sustainable development based on tourism: A case study of Slovak Rural Region, *Environmental Engineering and Management Journal*, **2017**, 2(16), 449–458. <https://doi.org/10.30638/eemj.2017.045>.

- [49] Klein, K.M., Lebanon mountain. – The Encyclopedia of Ancient History. R.S. Bagnall, K. Brodersen, C.B. Champion, A. Erskine and S.R. Huebner (eds.), **2012** <https://doi.org/10.1002/9781444338386.wbeah14180>.
- [50] Lamouroux, M., Le karst libanais: sols de karst et altérations des roches carbonatées. Mémoires et Documents, *Phénomènes karstiques*, **1974**, 15(2), 15–26. <http://www.documentation.ird.fr/hor/fdi:29456>.
- [51] Lemenkov, V.; Lemenkova, P., *Using TeX Markup Language for 3D and 2D Geological Plotting*, Foundations of Computing and Decision Sciences, **2021a**, 46(3), 43–69. <https://doi.org/10.2478/fcds-2021-0004>.
- [52] Lemenkov, V., Lemenkova, P., *Measuring Equivalent Cohesion C_{eq} of the Frozen Soils by Compression Strength Using Kriolab Equipment*, Civil and Environmental Engineering Reports, **2021b**, 31(2), 63–84. <https://doi.org/10.2478/ceer-2021-0020>.
- [53] Lemenkova, P., Seagrass Mapping and Monitoring Along the Coasts of Crete, Greece. M.Sc. Thesis. Netherlands: University of Twente, **2011**. <https://doi.org/10.13140/RG.2.2.16945.22881>.
- [54] Lemenkova, P.; Promper, C.; Glade, T., Economic Assessment of Landslide Risk for the Waidhofen a.d. Ybbs Region, Alpine Foreland, Lower Austria, In: Eberhardt, E., Froese, C., Turner, A. K. and Leroueil, S. (Eds.). Protecting Society through Improved Understanding. 11th International Symposium on Landslides & the 2nd North American Symposium on Landslides & Engineered Slopes (NASL), June 2–8, 2012. Canada, Banff, **2012**, 279–285. <https://doi.org/10.6084/m9.figshare.7434230>.
- [55] Lemenkova, P., Monitoring Changes in Agricultural Landscapes of Central Europe, Hungary: Application of ILWIS GIS for Image Processing, In: Geoinformatics: Theoretical and Applied Aspects. Ukraine, Kiev, May 13–16, **2013**. <https://doi.org/10.3997/2214-4609.20142479>.
- [56] Lemenkova, P., *Statistical Analysis of the Mariana Trench Geomorphology Using R Programming Language*, Geodesy and Cartography, **2019a**, 45(2), 57–84. <https://doi.org/10.3846/gac.2019.3785>.
- [57] Lemenkova, P., *Topographic surface modelling using raster grid datasets by GMT: example of the Kuril-Kamchatka Trench, Pacific Ocean*, Reports on Geodesy and Geoinformatics, **2019b**, 108, 9–22. <https://doi.org/10.2478/rgg-2019-0008>.
- [58] Lemenkova, P., *GMT Based Comparative Analysis and Geomorphological Mapping of the Kermadec and Tonga Trenches, Southwest Pacific Ocean*, Geographia Technica, **2019c**, 14(2), 39–48. https://doi.org/10.21163/GT_2019.142.04.
- [59] Lemenkova, P., Geomorphological modelling and mapping of the Peru-Chile Trench by GMT, *Polish Cartographical Review*, **2019d**, 51(4), 181–194. <https://doi.org/10.2478/pcr-2019-0015>.
- [60] Lemenkova, P., Using GMT for 2D and 3D Modeling of the Ryukyu Trench Topography, Pacific Ocean, *Miscellanea Geographica*, **2020a**, 25(3), 1–13. <https://doi.org/10.2478/mgrsd-2020-0038>.

- [61] Lemenkova, P., *Geomorphology of the Puerto Rico Trench and Cayman Trough in the Context of the Geological Evolution of the Caribbean Sea*, *Annales Universitatis Mariae Curie-Sklodowska, sectio B – Geographia, Geologia, Mineralogia et Petrographia*, **2020b**, 75, 115–141. <https://doi.org/10.17951/b.2020.75.115-141>.
- [62] Lemenkova, P., *Variations in the bathymetry and bottom morphology of the Izu-Bonin Trench modelled by GMT*, *Bulletin of Geography. Physical Geography Series*, **2020c**, 18(1), 41–60. <https://doi.org/10.2478/bgeo-2020-0004>.
- [63] Lemenkova, P., *GEBCO Gridded Bathymetric Datasets for Mapping Japan Trench Geomorphology by Means of GMT Scripting Toolset*, *Geodesy and Cartography*, **2020d**, 46(3), 98–112. <https://doi.org/10.3846/gac.2020.11524>.
- [64] Lemenkova, P., Geodynamic setting of Scotia Sea and its effects on geomorphology of South Sandwich Trench, Southern Ocean, *Polish Polar Research*, **2021a**, 42(1), 1–23. <https://doi.org/10.24425/ppr.2021.136510>.
- [65] Lemenkova, P., *The visualization of geophysical and geomorphologic data from the area of Weddell Sea by the Generic Mapping Tools*, *Studia Quaternaria*, **2021b**, 38(1), 19–32. <https://doi.org/10.24425/sq.2020.133759>.
- [66] Maalouf, R.P., Atlas du Liban. *Confins*, **2008**, 4, 5122. <https://doi.org/10.4000/confins.5122>.
- [67] Makhzoumi, J.; Chmaitelly, H.; Lteif, C., Holistic conservation of bio-cultural diversity incoastal Lebanon: A landscape approach, *Journal of Marine and Island Cultures*, **2012**, 1, 27–37. <http://dx.doi.org/10.1016/j.imic.2012.04.003>.
- [68] Maksoud, S., Granier, B.; Gèze, R.; Almèras, Y.; Toland, C.; Azar, D., The Jurassic/Cretaceous boundary in Lebanon. Revision of the Salima Formation, *Cretaceous Research*, **2020**, 107, 104268. <https://doi.org/10.1016/j.cretres.2019.10426>.
- [69] Mouterde, P., Nouvelle flore du Liban et de la Syrie. Dar el-Machreq, **1983**.
- [70] Nader, F., Swennen, R.; Ottenburgs, R., Karst-meteoric dedolomitization in Jurassic carbonates, Lebanon, *Geologica Belgica*, **2003**, 6(1–2), 3–23. URL: <https://popups.uliege.be/1374-8505/index.php?id=2086>.
- [71] Nakhoul, J., Fernandez, C.; Bousquet-Mélou, A.; Nemer, N.; Abboud, J.; Prévosto, B., Vegetation dynamics and regeneration of *Pinus pinea* forests in Mount Lebanon: Towards the progressive disappearance of pine, *Ecological Engineering*, **2020**, 152, 105866. <https://doi.org/10.1016/j.ecoleng.2020.105866>.
- [72] Nassif, M.-H., Groundwater Governance in the Central Bekaa Lebanon, Technical Report, 130 p., **2016**.

- [73] Nicod J.; Sanlaville, P., Etude géomorphologique de la région littorale libanaise, In: *Méditerranée, deuxième série*, **1978**, 1–2, 134–135. https://www.persee.fr/doc/medit_0025-8296_1978_num_32_1_1778.
- [74] Pasquier J., De la patrimonialisation du karst libanais: étude du site Unesco de la vallée de la Qadisha, Nord-Liban, *Karstologia: revue de karstologie et de spéléologie physique, Le karst du Yucatan (Mexique)*, **2010**, 55, 39-48. <https://doi.org/10.3406/karst.2010.2669>.
- [75] Pollastro, R.M.; Karshbaum, A.S.; Viger, R.J., Maps showing geology, oil and gas fields and geologic provinces of the Arabian Peninsula, *U.S. Geological Survey Open-File Report*, **1999**, 97-470-B: 14. <https://doi.org/10.3133/ofr97470B>.
- [76] QGIS.org, QGIS Geographic Information System. QGIS Association. <http://www.qgis.org> **2021**.
- [77] R Core Team, R: A language and environment for statistical computing, R Foundation for Statistical Computing, Vienna, Austria. URL: <https://www.R-project.org/> **2020**.
- [78] RStudio Team, RStudio: Integrated Development Environment for R. RStudio, Inc., Boston, MA. <https://www.RStudio.com/> **2017**.
- [79] Salah, M.K.; Alqudah, M.; David, C., Petrophysical and acoustic assessment of carbonate rocks, Zahle area, central Lebanon, *Bulletin of Engineering Geology and the Environment*, **2020**, 79, 5455–5475. <https://doi.org/10.1007/s10064-020-01900-0>.
- [80] Schenke, H.W.; Lemenkova, P., Zur Frage der Meeresboden-Kartographie: Die Nutzung von AutoTrace Digitizer für die Vektorisierung der Bathymetrischen Daten in der Petschora-See, *Hydrographische Nachrichten*, **2008**, 81, 16–21. <https://doi.org/10.6084/m9.figshare.7435538>.
- [81] Shaban, A., Analyzing climatic and hydrologic trends in Lebanon, *Journal of Environmental Science and Engineering*, **2011**, 3(5), 483–492.
- [82] Shaban, A., Geomorphological and Geological Aspects of Wetlands in Lebanon, In: The 3rd International Geography Symposium, Kemer-Antalya, Turkey, 10-13 June 2013. Abstract, **2013**.
- [83] Shaban, A.; Darwich, T.; El Hage, M., Studying Snowpack-Related Characteristics on Lebanon Mountains, *International Journal of Water Sciences* 1–11, **2013**. <https://doi.org/10.5772/57435>.
- [84] Shaban, A.; Drapeau, L.; Telesca, L.; Amacha, N.; Ghandour, A., Influence of snow cover on water capacity in the Qaraaoun Reservoir, Lebanon, *Arabian Journal of Geosciences*, **2021**, 14, 1–10. <https://doi.org/10.1007/s12517-020-06295-6>.
- [85] Suetova, I.A.; Ushakova, L.A.; Lemenkova, P., Geoinformation mapping of the Barents and Pechora Seas, *Geography and Natural Resources*, **2005**, 4, 138–142. <https://doi.org/10.6084/m9.figshare.7435535>
- [86] Tennekes, M., tmap: Thematic Maps in R, *Journal of Statistical Software*, **2012**, 84(6), 1–39, 2018.

- [87] Verdeil, E., Faour, G.; Hamzé, M., Atlas du liban. Les nouveaux défis. 2nd Ed. IFPO/CNRS Liban. ISBN: 978-2-35159-717-0, 106 pp., **2016**.
- [88] Veyret P.; de Vaumas, E., Le Liban (Montagne libanaise, Bekaa, Anti-Liban, Hermou, Haute Galilée libanaise). Etude de géographie physique, *Revue de géographie alpine*, **1955**, 43(4), 859–860. https://www.persee.fr/doc/rga_0035-1121_1955_num_43_4_1207_t1_0859_0000_1.
- [89] Walley, C., The Lithostratigraphy of Lebanon: A Review, *Lebanese Scientific Research Reports*, **1997**, 10(1), 81–108.
- [90] Walley, C.D., Some outstanding issues in the geology of Lebanon and their importance in the tectonic evolution of the Levantine region, *Tectonophysics*, **1998**, 298(1–3), 37–62. [https://doi.org/10.1016/S0040-1951\(98\)00177-2](https://doi.org/10.1016/S0040-1951(98)00177-2).
- [91] Wessel, P.; Luis, J.F.; Uieda, L.; Scharroo, R.; Wobbe, F.; Smith, W.H.F.; Tian, D., The Generic Mapping Tools version 6, *Geochemistry, Geophysics, Geosystems*, **2019**, 20, 5556–5564. <https://doi.org/10.1029/2019GC008515>.